Geosci. Model Dev. Discuss., doi:10.5194/gmd-2015-262, 2016
Manuscript under review for journal Geosci. Model Dev.
Published: 28 January 2016

Geoscientific Model Development Discussions
Open Access

Earth System Modelling on System-level Heterogeneous Architectures: EMAC (version 2.42) on the Dynamical Exascale Entry Platform (DEEP)

M. Christou[1], T. Christoudias[1], J. Morillo[2], D. A. Mallon[3] and H. Merx[1, 4]

[1]{The Cyprus Institute, Nicosia, Cyprus}

[2]{Barcelona Supercomputing Center, Barcelona, Spain}

[3]{Jülich Supercomputing Centre, Jülich, Germany}

[4]{Max Planck Institute for Chemistry, Mainz, Germany}

Correspondence to: T. Christoudias (christoudias@cyi.ac.cy)

Abstract

We examine an alternative approach to heterogeneous cluster-computing in the many-core era for Earth System models, using the European Centre for Medium-Range Weather Forecasts Hamburg (ECHAM)/Modular Earth Submodel System (MESSy) Atmospheric Chemistry (EMAC) model as a pilot application on the Dynamical Exascale Entry Platform (DEEP). A set of autonomous coprocessors interconnected together, called Booster, complements a conventional HPC Cluster and increases its compute performance, offering extra flexibility to expose multiple levels of parallelism and achieve better scalability. The EMAC model atmospheric chemistry code (Module Efficiently Calculating the Chemistry of the Atmosphere (MECCA)) was taskified with an offload mechanism implemented using OmpSs directives. The model was ported to the MareNostrum 3 supercomputer to allow testing with Intel Xeon Phi accelerators on a production-size machine. The changes proposed in this paper are expected to contribute to the eventual adoption of Cluster-Booster division and Many Integrated Core (MIC) accelerated architectures in presently available implementations of Earth System Models, towards exploiting the potential of a fully Exascale-capable platform.

Geosci. Model Dev. Discuss., doi:10.5194/gmd-2015-262, 2016
Manuscript under review for journal Geosci. Model Dev.
Published: 28 January 2016

1 Introduction

The ECHAM/MESSy Atmospheric Chemistry (EMAC) model is a numerical chemistry and climate simulation system that includes sub-models describing tropospheric and middle atmosphere processes and their interaction with oceans, land and human influences (Jöckel et al., 2010). It uses the second version of the Modular Earth Submodel System (MESSy2) to link multi-institutional computer codes. The core atmospheric model is the 5th generation European Centre for Medium Range Weather Forecasts Hamburg general circulation model (ECHAM5, Roeckner et al., 2003, 2006).

The EMAC model runs on several platforms, but it is currently unsuitable for massively parallel computers, due to its scalability limitations and large memory requirements per core. EMAC employs complex Earth-system simulations, coupling a global circulation model (GCM) with local physical and chemical models. The global meteorological processes are strongly coupled and have high communication demands while the local physical processes are inherently independent with high computation demands. This heterogeneity between different parts of the EMAC model poses a major challenge when running on homogeneous parallel supercomputers.

We test a new approach for a novel supercomputing architecture as proposed by the DEEP project (Eicker et al., 2013, 2015, Mallon et al., 2012, 2013, Suarez et al, 2011), an innovative European response to the Exascale challenge. Instead of adding accelerator cards to Cluster nodes, the DEEP project proposes to use a set of interconnected coprocessors working autonomously (called Booster), which complements a standard Cluster. Together with a software stack focused on meeting Exascale requirements—comprising adapted programming models, libraries and performance tools—the DEEP architecture enables unprecedented scalability. The system-level heterogeneity of DEEP, as opposed to the common node-level heterogeneity, allows users to run applications with kernels of high scalability alongside kernels of low scalability concurrently on different sides of the system, avoiding at the same time over and under-subscription.

The Cluster–Booster architecture is naturally suited to global atmospheric circulation–chemistry models, with global components running on the Cluster nodes exploiting the high-speed Xeon processors and local components running on the highly-parallel Xeon Phi co-processors. By balancing communication versus computation the DEEP concept provides a new degree of freedom allowing us to distribute the different components at their optimal parallelisation. The concept is depicted diagrammatically in Figure 1.

2 Overview of application structure

The EMAC model comprises two parts, the meteorological base model ECHAM, using a nonlocal, spectral algorithm with low scalability, and the modular framework MESSy, linking local physical and chemical processes to the base model, with high scalability. While the number of processors used for the base model is limited by the non-local spectral representation of global physical processes, local physical and chemical processes described by framework submodels run independently from their neighbours and present very high scalability.

2.1 Phases

The implementation of EMAC comprises two main phases, the base model ECHAM integrating the dynamical state of the atmosphere, and the MESSy framework that interfaces to *n* submodels calculating physical and chemical processes. Among these submodels stands out the MECCA submodel (Sander et al., 2007). This submodel computes the chemical kinetics of the homogeneous gas-phase chemistry of the atmosphere, and deserves special mention due to its intrinsic parallelism, high computational demands, and load imbalance rising from its rigid coupling to the base model's parallel decomposition.

The ECHAM base model runs in parallel in the distributed-memory paradigm using the Message Passing Interface (MPI, Aoyama et al., 1999) library for communication; the MESSy framework inherits the parallel decomposition defined by the base model. While ECHAM has been shown to be able to exploit the shared-memory paradigm using the Open Multi-Processing (OpenMP) library (Dagum et al., 1998), no such effort had been undertaken for the MESSy model so far.

It is, however, currently not possible to delegate the whole MESSy subsystem to full multi-threaded execution as some physical processes are naturally modelled in a column-based approach, and are strongly dependent on the system states at their vertically adjacent grid points. The implementation of submodels simulating these processes consequently relies on the column structure inherited from the base model. Furthermore, even a coarser column-oriented multi-threaded approach is hindered by global-variable interdependencies between submodels.

Describing homogeneous gas phase chemical kinetics, the MESSy submodel MECCA executes independently of its physical neighbours and is not limited by vertical adjacency relations. As more than half of the total run-time is spent in MECCA for a typical model scenario, it seems adequate to concentrate on the MECCA kernel with strong algorithmic locality and small communication volume per task. As sketched in Figure **1** the current implementation of MECCA, developed in the DEEP project, is delegated to the Booster using a task-based approach while both ECHAM and the remaining MESSy submodels are executed on the Cluster in the distributed-memory paradigm.

2.2 Dominant factors

Implementing a spectral model of the dynamical state of the atmosphere, the ECHAM phase comprises six transform and six transposition operations in each time step, as seen in Figure 3. The data in memory for each time step (data size scales with the square of the model resolution) is transposed in an all-to-all communication pattern, and this phase is dominated by network bandwidth.

Figure 4 displays one time step traced with Extrae/Paraver (Extrae 2015, Paraver 2015) starting with the end of the grid point calculations of the last time step—in which most processors are already idle (orange) due to load imbalance and waiting for process 14 (blue) to finish running. This is followed by the transpositions and Fourier and Legendre transformations (magenta), which execute simultaneously as further analysis showed. After the transpositions a short interval with all processors running (blue) can be identified with the time step integration in spectral space, followed by the inverse transformations and transpositions and transport calculations in ECHAM.

While the pattern described so far repeats towards the end of the displayed interval, the major fraction of the time step is spent without communication, running (blue) or waiting (orange) in calculations in MESSy in grid space. The MESSy phase comprises some 30 submodels that are tightly coupled by exchanging the atmospheric observables using global variables. Model performance depends largely on a virtual longitude run-time parameter exploiting cache line adjacency of the grid point variables. Investigations during the first phase of the project determined the load imbalance visible in Figure 4 to be caused by chemical processes computed in the MECCA submodel.

The observed load imbalance is one of the main factors determining application scalability. It is caused by an adaptive time-step integrator solving a system of differential equations. As the stiffness of these equations representing homogeneous photochemical reactions varies by up to two orders of magnitude due to changes in the intensity of sunlight, the adaptive integrator demands varying amounts of run time accordingly (described in more detail in Section 2.3).

In the MECCA phase the algorithmically complex adaptive time-step differential equation integrator operates on chemical concentrations of a total data size of the order of a few kilobytes per grid point. Yet, as seen in Figure 5 that highlights the load imbalance caused by MECCA and observed using Scalasca (Scalasca 2015), this phase consumes the major proportion of the total execution time, it is compute-bound and an obvious candidate for offloading to accelerators. It should be noted though, that in a regular architecture, accelerating this highly parallel phase will not eliminate the load imbalance.

2.3 Scalability considerations

To test the model scalability out-of-the-box, the EMAC application has been ported to the JUDGE cluster at JSC, and a representative benchmark with a horizontal resolution of 128 grid points in longitudinal and 64 grid points in latitudinal direction with 90 vertical levels and a spin-up period of 8 simulated months has been compiled, frozen and packaged to be used for measurements. Table **1** details the experimental setup for the results shown in this section.

EMAC was benchmarked with different numbers of processors on JUDGE in order to determine the run time behaviour of the total application. As shown in Figure 6 the application scales up to 384 processes (16 nodes x 24 MPI processes each), at higher numbers the performance decreases. Parallel execution speed is determined by the balance of three factors: computation, communication, and load imbalance. The benchmarking setup for the JUDGE cluster can be seen in Table 2. While the computational resources increase with additional processors and therefore increase the application performance, communication demands diminish the positive effect of the additional processors. Additionally, increasing the granularity of the total workload also increases the load imbalance.

While the number of processors used for the distributed-memory part of the code is limited by the scalability of the non-local representation of global physical processes in ECHAM, the local processes in MESSy running independently from their neighbours scale very well. The MESSy subsystem has not been designed for multi-threaded execution, though, and contains non-local code due to characteristics of the physical processes and algorithmic design decisions. Some physical processes are naturally modelled in a column-based approach, because they are strongly dependent on the system states at vertically adjacent grid points, e.g. sunlight intensity at lower grid points depending on the absorption at higher grid points, and precipitation depending on the flux of moisture from vertically adjacent grid cells. Sub-models simulating these processes consequently rely on the column structure implemented in the current model.

In the existing distributed-memory parallel decomposition, the three-dimensional model grid is split horizontally using two run-time parameters, setting the number of processes in latitudinal and longitudinal direction. As work is distributed independently for each direction, a rectangular decomposition is obtained.

The physical load-imbalance, caused by photo-chemical processes in the lower stratosphere and natural and anthropogenic emissions, appears in the run time spent for each grid point when examining the benchmark calculations. In Figure 7 the maximal MECCA kernel execution wall-time for one grid point in each column differs by up to a factor of four. The load imbalance is caused by the adaptive time-step integrator solving the differential equations that describe the chemical equations computed in the MECCA submodel. The strongly varying light intensity at sunrise and sunset and night-time emissions lead to stiff differential equations that require more intermediate time steps with derivative function evaluations and increase the computational load by up to one order of magnitude.

At high levels of parallelisation, the load imbalance becomes a limiting factor, and the factors determining scalability in absolute numbers in Figure 8 are both communication and computation. For the ECHAM phase (blue), when scaling to beyond 8 nodes the communication demands of the underlying spectral model involving several all-to-all communication patterns start to dominate.

In Figure 9 the point at which communication and computation require equal times around 8 nodes is clearly apparent; 16 nodes is commonly used in production runs of the EMAC atmospheric model as a scientific application to balance efficiency and total required wall time.

3 Model Developments

3.1 Intranode taskification

The EMAC model atmospheric chemistry code (MECCA) was taskified using OmpSs (Bueno, J. et al., 2011, 2012, Duran, A. et al., 2011, Florentino et al., 2014) directives. OmpSs allows the user to specify inputs and outputs for blocks of code or functions, giving enough information to the runtime to construct a dependency graph. This dependency graph reflects at all moments which tasks are ready to be executed concurrently, and therefore the programmer does not have to explicitly manage the parallelisation. This idea of tasks and task dependencies has been adopted in the OpenMP 4.0 standard (OPENMP 4.0, 2013). Since in MECCA each gridpoint is completely independent of its neighbours, this part of the code is in principle embarrassingly parallel, with no communication or inter-task dependencies involved.

The MECCA submodel was refactored through the creation of computational kernels for intranode parallelisation with shared-memory tasks. The new version of EMAC, running ECHAM with MPI processes and MECCA with shared-memory OmpSs tasks outperforms the old EMAC using pure MPI, and continues to scale beyond the region where the original implementation scaling performance plateaus. This can be seen in Figure 10, which shows the performance using multi-threading on the DEEP Cluster.

3.2 Internode taskification

In DEEP, OmpSs has been extended to support offloading tasks to remote nodes (Beltran et al., 2015). This mimics the behaviour of other accelerator APIs that move data from the host to the device, compute in the device, and return the results to the host. However, OmpSs adds two very important features: i) it allows offloading to remote nodes, not just locally available coprocessors/accelerators, which is a key functionality to effectively use the Booster; and ii) it allows using the Booster as a pool of coprocessors, so tasks can be offloaded to any Booster node with enough free cores. The latter enables to eliminate the load-imbalance caused by sunlight gradients in MECCA.

In a shared-memory taskification the data is already shared between threads, and no memory copies are necessary. However, in DEEP, to leverage the Booster, this data has to be copied to the Booster nodes. Keeping that in mind, the new task-based MECCA implementation was optimised and the memory and network footprint of the distributed-memory offloading was reduced by three orders of magnitude. To minimise the memory footprint for offloaded tasks, the number of computational grid elements issued to MESSy is further split into individual elements for each task, by rearranging the grid point arrays in each time step to implement data locality at the grid-point level, resulting in a reduction of the total memory footprint from 2.7 MB down to 6.3 KB for each task. This was the result of refactoring both the data and code structures in MECCA. At the benchmark resolution of T42L90MA a total number of 737 280 tasks are generated in each time.

As discussed in section 2.2, a detailed analysis of the EMAC run-time behaviour using Scalasca (Wolf et al., 2008) and Extrae/Paraver has identified that the MECCA submodel consumes a major proportion of the execution time, does not participate in communication, and is independent of adjacency constraints. It is thus well suited to be delegated to the Booster employing the large dynamical pool of accelerator resources provided by the DEEP concept for load balancing of the heavily varying computation demands discussed in section 2.3.

Additionally, the distributed-memory offloading code was redesigned to exploit shared memory within the Xeon Phi many-core processors by nesting an OmpSs shared-memory region within Cluster-to-Booster tasks encompassing variable, runtime-defined number of individual gridpoint calculations. Thus, the number of tasks to be sent to the Booster can be controlled and optimised for each architecture, and host-specific configuration allows for optimum task size based on bandwidth, reducing task communication overheads.

With this approach, the specifics of the DEEP system architecture, and in particular the hardware present in MIC coprocessors is exploited by massively parallelising the chemistry calculations at the gridpoint level and offloading to the Booster exposing a significant amount of thread parallelism. At the same time the load imbalance observed in MECCA is automatically alleviated through OmpSs' dynamic load balancing by selecting a sufficiently fine task size and decoupling the model-domain location of the grid point from the task execution on the physical CPU.

3.3 Vectorisation

The computational core of MECCA is connected by an interface layer to the MESSy framework, integrating different submodel code and data structures into the ECHAM base model. It provides the gridpoint data as sub-arrays of the global simulation data – which have been rearranged from their native longitude and latitude coordinates into a virtual longitude and an outer index variable counting the virtual longitude blocks and assuming the role of a virtual latitude. The virtual longitude exploits cache line adjacency on non-vector architectures and serves as run-time vectorisation parameter for all MESSy submodels.

For the MECCA submodel an integrator kernel has been created that can be offloaded onto worker threads running on the main processor or hardware accelerators. The chemical mechanism is compiled by the Kinetic Pre-processor (KPP, Damian et al., 2002) implementing a domain-specific language for chemical kinetics. The integrator kernel operates on the

Geosci. Model Dev. Discuss., doi:10.5194/gmd-2015-262, 2016
Manuscript under review for journal Geosci. Model Dev.
Published: 28 January 2016

variables of one grid-point describing the local state of the atmosphere and the integrator parameters determining the solution of the chemical equations. As the kernel variables are passed as one-dimensional sub-arrays of global, four-dimensional arrays, extending along the virtual longitude, the vector variables are transposed to extend contiguously along the dimension of chemical species.

In order to estimate the run-time effect of the changes in the code, the application was benchmarked on the DEEP Cluster using the Xeon main processors without vectorisation as baseline measurement of 548.65 seconds per simulated day. Compiling with the auto-vectoriser enabled for the AVX instruction set extensions decreased the run time to 466.40 seconds, resulting in a first speed-up of 1.18. Examination of the optimisation report identified several unaligned array accesses, which were solved using compiler directives and introducing aligned leading dimensions at 64-byte boundaries for multi-dimensional arrays as needed for the instruction set of Intel Xeon Phi. These changes improved the total application performance to 349.50 seconds per simulated day for a second speed-up of 1.33 achieving a total speed-up of 1.57 (Figure 11).

4 Attainable Performance

At the time of writing this manuscript the DEEP Booster is in the bring-up phase, and not available to users. In order to project the performance of the full DEEP System, Xeon-based measurements on the DEEP Cluster were combined with Xeon Phi-based measurements on MareNostrum 3. The DEEP Cluster reference data weighted by the relative factors for each phase derived from the metrics measurements exhibit a performance maximum for the base model (ECHAM) and MESSy (excluding MECCA) at 8 nodes, representing a good estimate for the optimal parallelisation of that phase on the Cluster. This estimate of 375 s per simulated day for the low-scaling Cluster phases was used to extrapolate the attainable performance, merging this result at 8 nodes, with the Xeon Phi data retrieved from MareNostrum 3, where benchmarks using one node had been run with varying numbers of processing elements within one Xeon Phi processor. The pure MPI time in the DEEP Cluster, the time for each phase, and the theoretical performance when offloading to the Booster are shown in Figure 12.

While the number of Booster nodes required to attain similar performance to the original distributed-memory based implementation corresponds to regular accelerator architectures with individual boosters directly attached to cluster nodes, the projected DEEP performance scales beyond the optimal performance achieved so far. The EMAC atmospheric chemistry global climate model seems therefore well suited to exploit an architecture providing considerable more hardware acceleration than provided by regular systems. The projected attainable performance that outperforms the pure-MPI conventional cluster paradigm at higher core count (depicted here as the number of Booster nodes, while keeping the ECHAM/MESSy MPI part on 8 Cluster nodes for optimal performance) is also shown in Figure **12**.

5 Conclusions

The global climate model ECHAM/MESSy Atmospheric Chemistry (EMAC) is used to study climate change and air quality scenarios. The EMAC model is constituted by a nonlocal meteorological part with low scalability, and local physical/chemical processes with high scalability. The model's structure naturally suits the DEEP Architecture using the Cluster nodes for the nonlocal part and the Booster nodes for the local processes. Different implementations of the code's memory and workload divisions were developed and benchmarked to test different aspects of the achievable performance on the proposed architecture. The use of the OmpSs API largely frees the programmers of implementing the offloading logic and, given that EMAC is developed and used in a large community working on all aspects of the model, can facilitate adoption of the concept in the MESSy community.

The chemistry mechanism was taskified at the individual gridpoint level using OmpSs directives. The chemistry code was refactored to allow for memory adjacency of vector elements. Enabling the vectoriser achieves a total speed-up of 1.57 by aligning all arrays at 64-byte boundaries. The OmpSs taskification with remote offload allows for massive task parallelisation and the implementation of optional two-stage offload to control Cluster-Booster task memory size and optimum bandwidth utilisation.

The computational load imbalance arising from a photochemical imbalance is alleviated at moderate parallelisation by assigning grid points with differing run times to each process and distributing the load over all processes. Due to the physical distribution of sunlight this load balancing does not require an explicit algorithm at moderate parallelisation; instead, the implicit assignment of the model grid in rectangular blocks suffices for this purpose. At higher numbers of processors this implicit load-balancing decreases and the resulting load imbalance has to be solved by active balancing. The dynamic scheduling provided by the OmpSs run-time system balances the computational load without a possible, but expensive prediction for the current time step.

With these approaches, the specifics of the DEEP System architecture, and in particular the hardware present in MIC coprocessors can be exploited by massively parallelising the chemistry calculations at the gridpoint level and offloading to the Booster exposing a significant amount of thread parallelism. At the same time the load imbalance observed in MECCA will be automatically alleviated through dynamic load balancing by selecting a sufficiently fine task size and decoupling the model-domain location of the cell from the task execution on the physical CPU.

Benchmark projections based on available hardware running the DEEP software stack suggest that the EMAC model requires the large numbers of Xeon Phi accelerators available in the DEEP architecture to scale beyond the current optimal performance point and exploit Amdahl's law with the highly scalable gridpoint calculations while capitalising on the high performance and fast communication for the spectral base model on Intel Xeon processors.

The changes proposed in this paper are expected to contribute to the eventual adoption of MIC accelerated architectures for production runs, in presently available implementations of Earth System Models, towards exploiting the potential of a fully Exascale-capable platform.

Code Availability

The Modular Earth Submodel System (MESSy) is continuously further developed and applied by a consortium of institutions. The usage of MESSy and access to the source code is licenced to all affiliates of institutions which are members of the MESSy Consortium. Institutions can become a member of the MESSy Consortium by signing the MESSy Memorandum of Understanding. More information can be found on the MESSy Consortium Website (http://www.messy-interface.org).

Acknowledgements

The research leading to these results has received funding from the European Community's Seventh Framework Programme (FP7/2007-2013) under Grant Agreement n° 287530.

References

Aoyama, Y. and Nakano, J., *RS/6000 SP: Practical MPI Programming*, 1999.

Beltran, V., Labarta, J. and Sainz, F., *Collective Offload for Heterogeneous Clusters*, IEEE International High Performance Computing (HiPC), Bangalore, India, 2015.

Bueno, J., Planas, J., Duran, A., Badia, R.M., Martorell, X., Ayguade, E. and Labarta, J., *Productive Programming of GPU Clusters with OmpSs*, Parallel & Distributed Processing Symposium (IPDPS), 2012 IEEE 26th International, 557–568, 2012.

Bueno J., Martinell L., Duran A., Farreras M., Martorell X., Badia R. M., Ayguade E. and Labarta J., *Productive cluster programming with OmpSs*, Euro-Par 2011 Parallel Processing, Lecture Notes in Computer Science **6852**, 555–566, 2011.

Dagum, L. and Menon, R.: OpenMP: an industry standard API for shared-memory programming, Computational Science & Engineering, IEEE **5**, 1, 46–55, 1998.

Damian, V., Sandu, A., Damian, M., Potra, F. and Carmichael, G.R.: *The Kinetic PreProcessor KPP—A Software Environment for Solving Chemical Kinetics*, Computers and Chemical Engineering **26**, 11, 1567–1579, 2002.

Duran, A., Ayguadé, E., Badia, R., M., Labarta, J., Martinell, L., Martorell, X., and Planas, J., *OmpSs: a proposal for programming heterogeneous multi-core architectures*, Parallel Processing Letters **21**, No. 02, 173–193, 2011.

Eicker, N., Lippert, T., Moschny, T. and Suarez, E., *The DEEP project: Pursuing cluster-computing in the many-core era*, Proc. of the 42nd International Conference on Parallel Processing Workshops (ICPPW) 2013, Workshop on Heterogeneous and Unconventional Cluster Architectures and Applications (HUCAA), Lyon, France, 885–892, 2013.

Eicker, N., Lippert, T., Moschny, T. and Suarez, E., *The DEEP Project—An alternative approach to heterogeneous cluster-computing in the many-core era*, Concurrency and Computation, 2015.

Extrae, Barcelona Supercomputing Center, https://www.bsc.es/computer-sciences/extrae, Last Access: 23/11/2015.

Florentino, S., Mateo, S., Beltran, V., Bosque, J., L., Martorell, X. and Ayguadé, E., *Leveraging OmpSs to Exploit Hardware Accelerators*, International Symposium on Computer Architecture and High Performance Computing, 112–119., 2014.

Jöckel, P., Kerkweg, A., Pozzer, A., Sander, R., Tost, H., Riede, H., Baumgaertner, A., Gromov S. and Kern, B., *Development cycle 2 of the Modular Earth Submodel System (MESSy2)*, Geoscientific Model Development **3**, 717–752, 2010.

Mallon, A, D., Lippert, T., Beltran, V., Affinito, F., Jaure, S., Merx, H., Labarta, J., Staffelbach, G, Suarez, E. and Eicker, N., *Programming Model and Application Porting to the Dynamical Exascale Entry Platform (DEEP)*, Proceedings of the Exascale Applications and Software Conference, Edinburgh, Scotland, UK., 2013.

Mallon, A., D., Eicker, N., Innocenti, M.E., Lapenta, G., Lippert, T. and Suarez, E., *On the Scalability of the Cluster-Booster Concept: a Critical Assessment of the DEEP Architecture*, FutureHPC '12, Proceedings of the Future HPC Systems: the Challenges of Power-Constrained Performance, ACM New York, 2012.

OpenMP Application Program Interface Version 4.0 – July 2013, OpenMP Architecture Review Board, http://www.openmp.org/mp-documents/OpenMP4.0.0.pdf, Last Access: 23/11/2015.

Paraver, Barcelona Supercomputing Center, https://www.bsc.es/computer-sciences/performance-tools/paraver, Last Access: 23/11/2015.

Roeckner, E., Brokopf, R., Esch, M., Giorgetta, M., Hagemann, S., Kornblueh, L., Manzini, E., Schlese, U. and Schulzweida, U., *Sensitivity of simulated climate to horizontal and vertical resolution in the ECHAM5 atmosphere model*, J. Climate **19**, 3771–3791, 2006.

Roeckner, E., Bäuml, G., Bonaventura, L., Brokopf, R., Esch, M., Giorgetta, M., Hagemann, S., Kirchner, I., Kornblueh, L., Manzini, E., Rhodin, A., Schlese, U., Schulzweida, U. and Tompkins, A., *The atmospheric general circulation model ECHAM 5. PART I: Model description*, Report/MPI für Meteorologie **349**, 2003.

Sander, R., Baumgaertner, A., Gromov, S., Harder, H., Jöckel, P., Kerkweg, A., Kubistin, D., Regelin, E., Riede, H., Sandu, A., Taraborrelli, D., Tost, H. and Xie, Z.-Q., *The atmospheric* *chemistry box model CAABA/MECCA-3.0,* Geoscientific Model Development **4**, 373–380, 2011.

Scalasca, http://www.scalasca.org/, Last Access: 23/11/2015.

Suarez, E., Eicker, N. and Gürich, W., *Dynamical Exascale Entry Platform: the DEEP Project*, inSiDE **9**, 2, 2011.

Table 1: Experimental setup for JUDGE scalability test out-of-the-box.

Scaling	Number of columns	Number of grid points	Number of chemical species	Spectral resolution
Strong scaling	8192 columns with 90 levels	737280 grid points	139 species in 318 reactions	T42L90MA with 42 coefficients

Table 2: System setup details for the analysis done on the JUDGE system.

Backend compiler version	MPI runtime version	Compilation flags	MPI processes per node
Intel 13.1.3	Parastation/Intel MPI 5.0.27	-O3 –fp-model source –r8 –align all	24

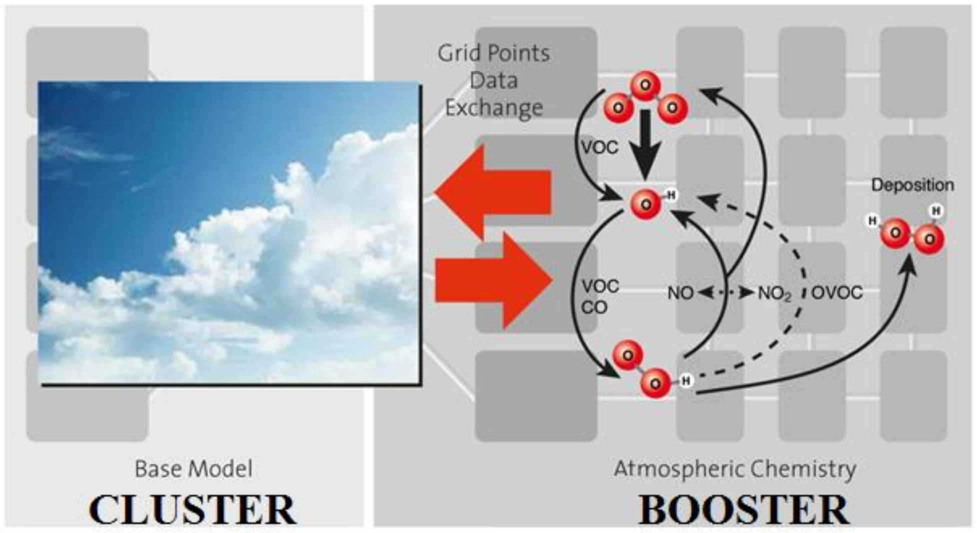

Figure 1 : Distribution of the Earth System Model components on the Cluster-Booster architecture.

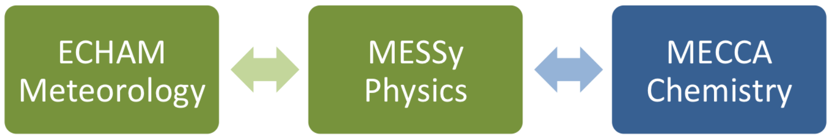

Figure 2 Phases of EMAC. Green phases run on the Cluster, blue phases run on the Booster.

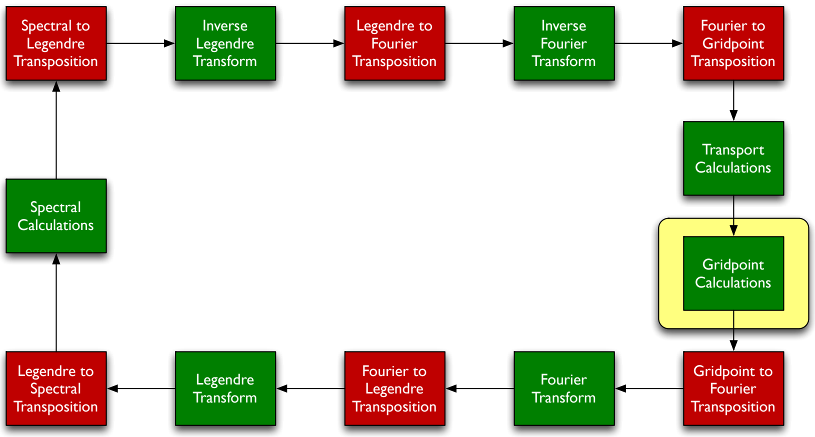
Spectral to Legendre Transposition
Inverse Legendre Transform
Legendre to Fourier Transposition
Inverse Fourier Transform
Fourier to Gridpoint Transposition
Transport Calculations
Gridpoint Calculations
Gridpoint to Fourier Transposition
Fourier Transform
Fourier to Legendre Transposition
Legendre Transform
Legendre to Spectral Transposition
Spectral Calculations

Figure 3 : The ECHAM main application loop. MESSy replaces and enhances the grid point calculations marked in yellow.

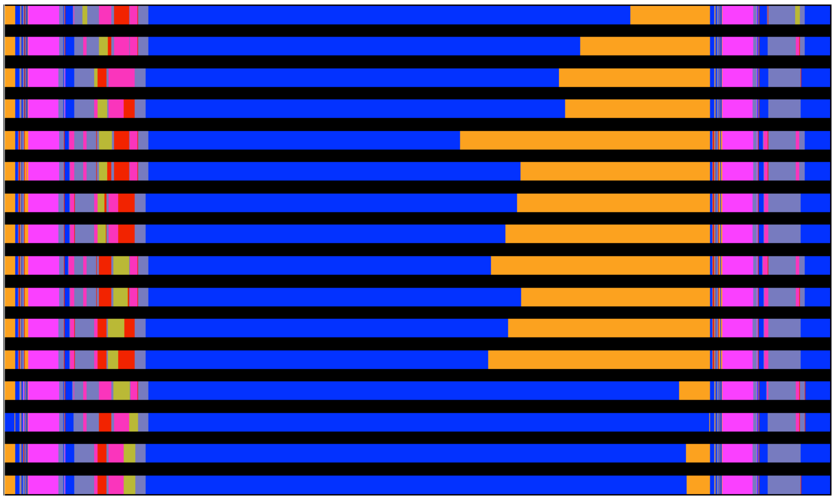

Figure 4 : Paraver trace of major processor usage of one time step. Time is along the horizontal and each bar corresponds to a separate CPU core. Blue colour depicts computation; orange corresponds to idle time due to load imbalance. The grid-space transpositions and Fourier and Legendre transformations are shown in magenta.

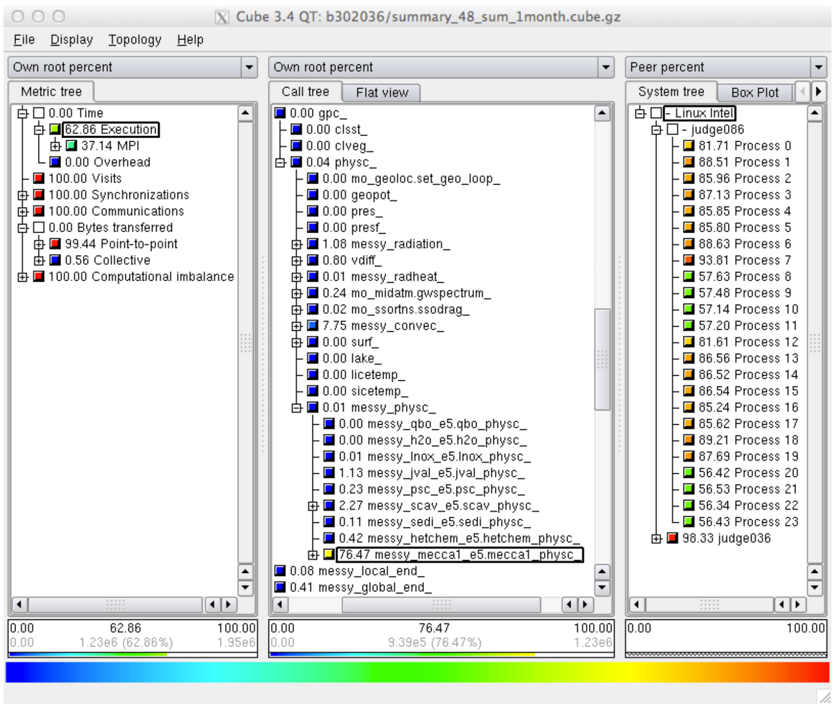
Cube 3.4 QT: b302036/summary_48_sum_1month.cube.gz

File Display Topology Help

```
Own root percent                 Own root percent                              Peer percent
Metric tree                      Call tree | Flat view                         System tree | Box Plot
0.00 Time                        0.00 gpc_                                     - Linux Intel
  62.86 Execution                  0.00 clsst_                                   - judge086
    37.14 MPI                      0.00 clveg_                                     81.71 Process 0
  0.00 Overhead                    0.04 physc_                                     88.51 Process 1
100.00 Visits                        0.00 mo_geoloc.set_geo_loop_                  85.96 Process 2
100.00 Synchronizations              0.00 geopot_                                  87.13 Process 3
100.00 Communications                0.00 pres_                                    85.85 Process 4
0.00 Bytes transferred               0.00 presf_                                   85.80 Process 5
  99.44 Point-to-point               1.08 messy_radiation_                         88.63 Process 6
  0.56 Collective                    0.80 vdiff_                                   93.81 Process 7
100.00 Computational imbalance       0.01 messy_radheat_                           57.63 Process 8
                                     0.24 mo_midatm.gwspectrum_                    57.48 Process 9
                                     0.02 mo_ssortns.ssodrag_                      57.14 Process 10
                                     7.75 messy_convec_                            57.20 Process 11
                                     0.00 surf_                                    81.61 Process 12
                                     0.00 lake_                                    86.56 Process 13
                                     0.00 licetemp_                                86.52 Process 14
                                     0.00 sicetemp_                                86.54 Process 15
                                     0.01 messy_physc_                             85.24 Process 16
                                       0.00 messy_qbo_e5.qbo_physc_                85.62 Process 17
                                       0.00 messy_h2o_e5.h2o_physc_                89.21 Process 18
                                       0.01 messy_lnox_e5.lnox_physc_              87.69 Process 19
                                       1.13 messy_jval_e5.jval_physc_              56.42 Process 20
                                       0.23 messy_psc_e5.psc_physc_                56.53 Process 21
                                       2.27 messy_scav_e5.scav_physc_              56.34 Process 22
                                       0.11 messy_sedi_e5.sedi_physc_              56.43 Process 23
                                       0.42 messy_hetchem_e5.hetchem_physc_      98.33 judge036
                                       76.47 messy_mecca1_e5.mecca1_physc_
                                   0.08 messy_local_end_
                                   0.41 messy_global_end_

0.00      62.86         100.00   0.00      76.47          100.00   0.00               100.00
0.00  1.23e6 (62.86%)   1.95e6   0.00  9.39e5 (76.47%)    1.23e6
```

Figure 5 : MECCA execution time analysed with Scalasca.

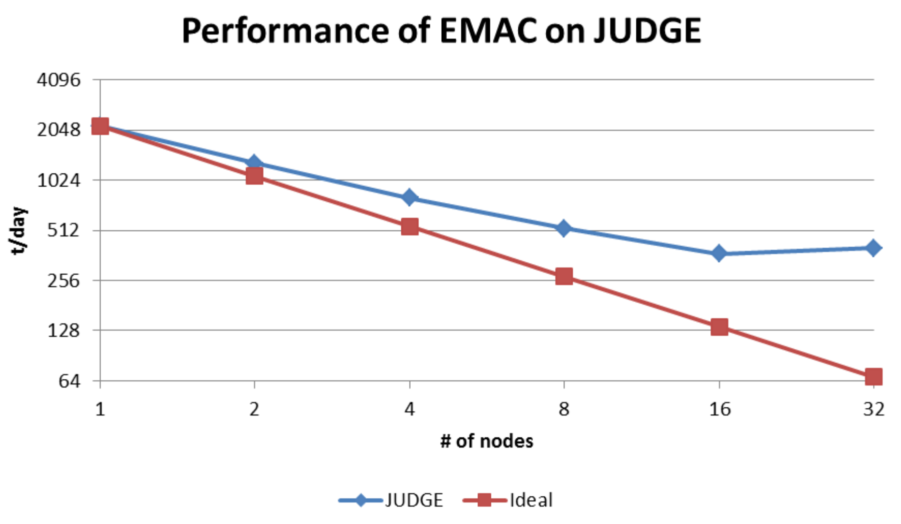

Figure 6 : Wall time for one simulated day versus the number of nodes on JUDGE.

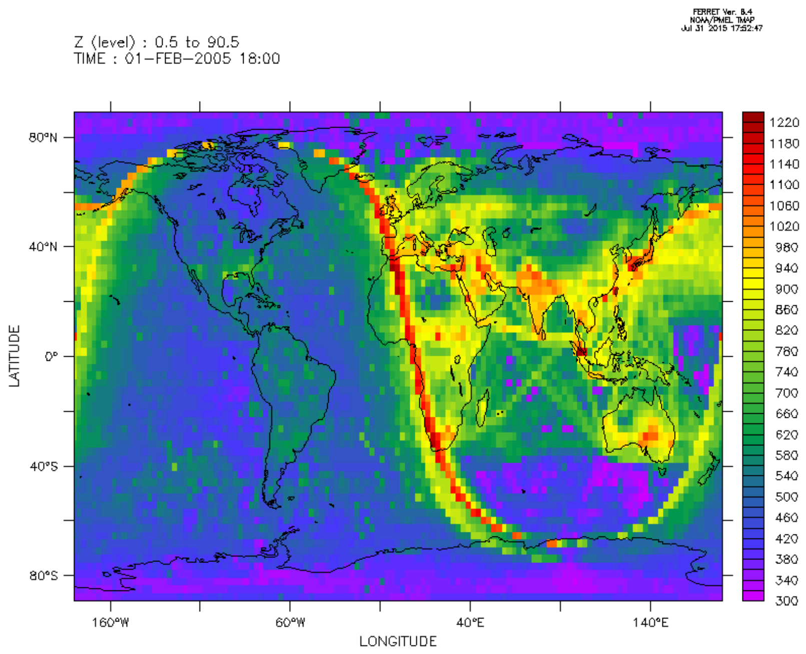

Figure 7 : Maximal MECCA kernel execution wall-time in microseconds. The adaptive time-step integrator shows a non-uniform run time caused by stratospheric photochemistry and natural and anthropogenic emissions.

Geosci. Model Dev. Discuss., doi:10.5194/gmd-2015-262, 2016
Manuscript under review for journal Geosci. Model Dev.
Published: 28 January 2016

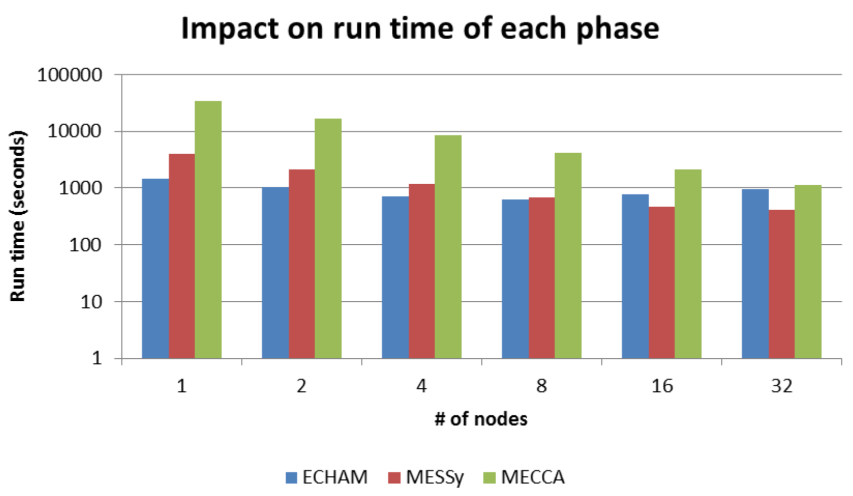

1

2 Figure 8 : Impact on run time of each phase of EMAC, when running on MareNostrum 3.

3

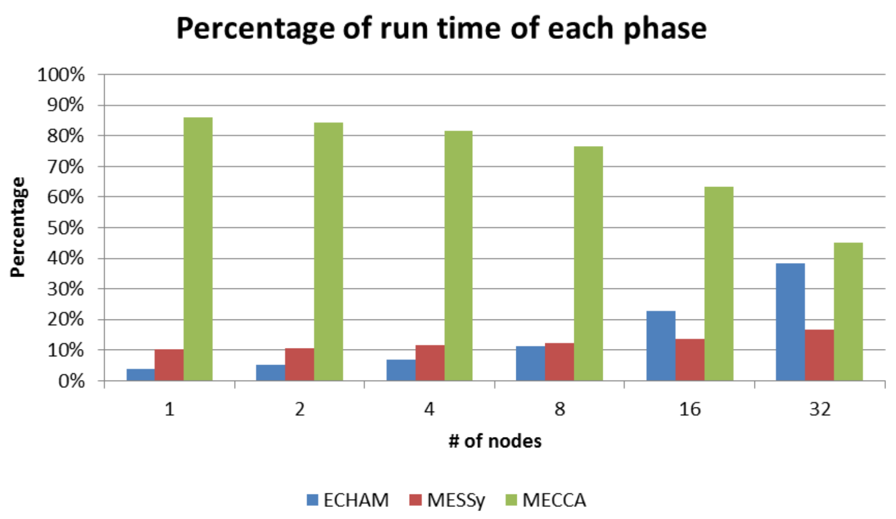

1

2 Figure 9 : Percentage of run time of each phase of EMAC, when running on MareNostrum 3.

3

Geosci. Model Dev. Discuss., doi:10.5194/gmd-2015-262, 2016
Manuscript under review for journal Geosci. Model Dev.
Published: 28 January 2016

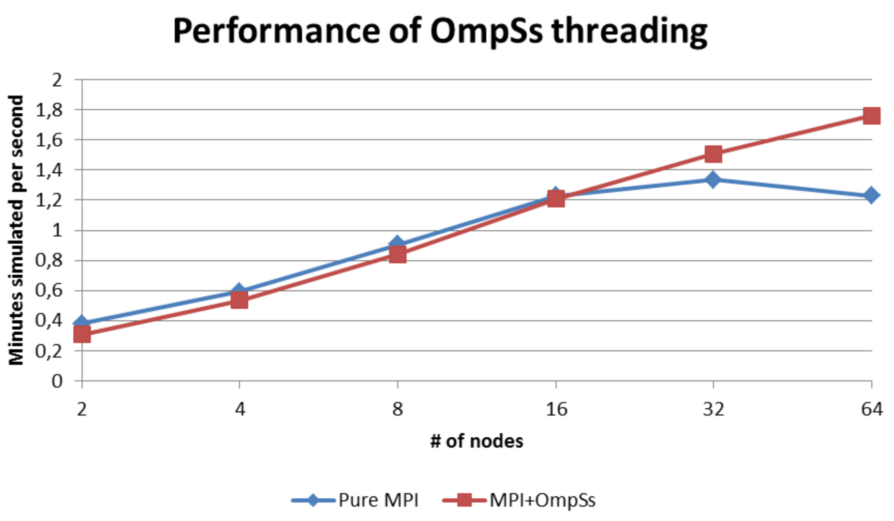

Figure 10 : Performance of OmpSs threading in the DEEP Cluster.

Geosci. Model Dev. Discuss., doi:10.5194/gmd-2015-262, 2016
Manuscript under review for journal Geosci. Model Dev.
Published: 28 January 2016

Geoscientific
Model Development
Discussions
Open Access

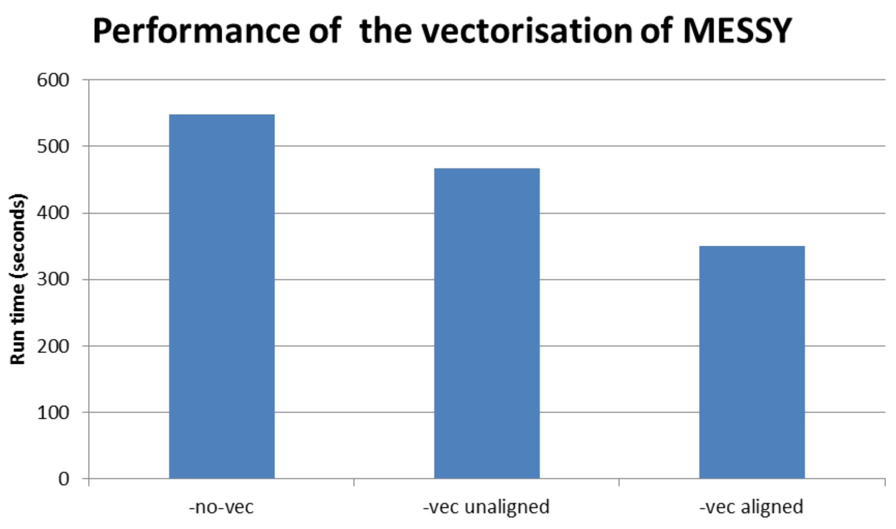

Figure 11 : Performance of the vectorisation of MESSY in a Xeon E5-2680.

Geosci. Model Dev. Discuss., doi:10.5194/gmd-2015-262, 2016
Manuscript under review for journal Geosci. Model Dev.
Published: 28 January 2016

1 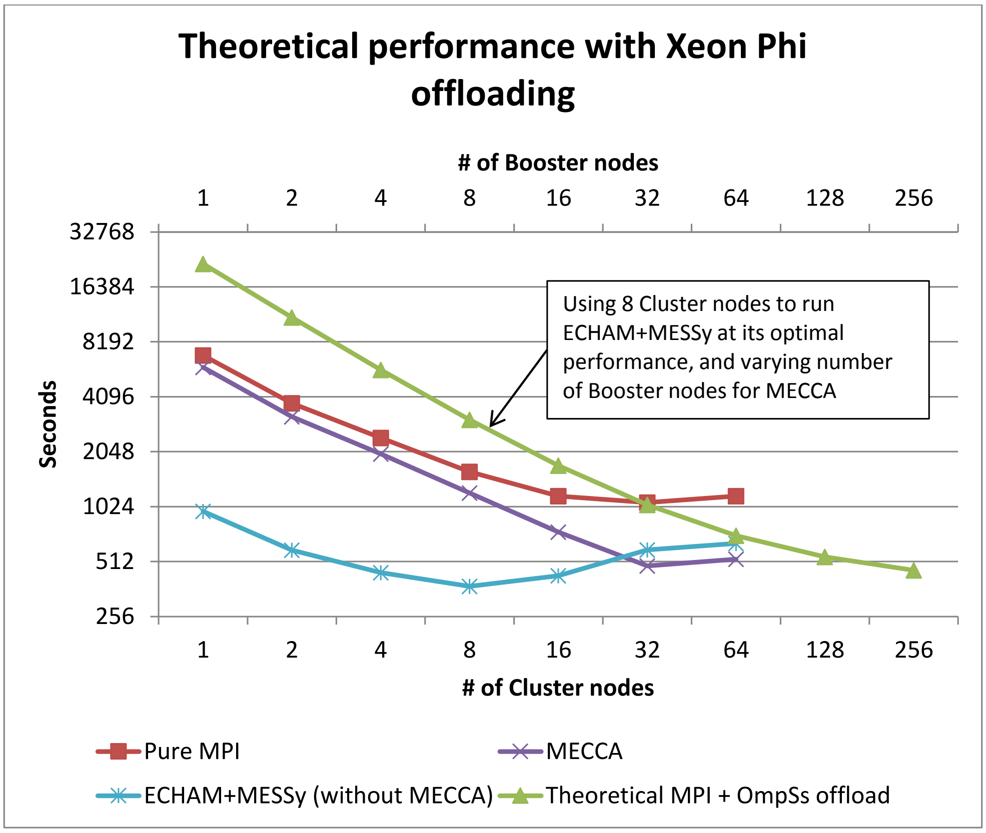

2 Figure 12: Time per simulated day in DEEP using a pure MPI approach, and a theoretical performance with
3 offloading to Xeon Phi, based on the metrics collected in MareNostrum 3. The theoretical MPI + OmpSs offload
4 data is based on a fixed configuration on the Cluster using 8 nodes, and scaling the number of Booster nodes.